ELSEVIER

Journal of Electromyography and Kinesiology 8 (1998) 93–100

JOURNAL OF ELECTROMYOGRAPHY AND KINESIOLOGY

Musculoskeletal balance of the human wrist elucidated using intraoperative laser diffraction

Richard L. Lieber [a,*], Jan Friden [b]

[a] *Departments of Orthopaedics and Bioengineering, Biomedical Sciences Graduate Group, University of California and Veterans Administration Medical Centers, San Diego, CA 92161, U.S.A.*

[b] *Department of Hand Surgery, Goteborg University, Goteborg, Sweden*

Abstract

This review describes a series of experiments in which sarcomere length was measured in human wrist muscles to understand their design. Sarcomere length measurements were combined with studies on cadaveric extremities to generate biomechanical models of human wrist function and to provide insights into the mechanism by which wrist strength balance is achieved. Intraoperative measurements of the human extensor carpi radialis brevis (ECRB) muscle during wrist joint rotation reveal that this muscle appears to be designed to operate on the descending limb of its length–tension curve and generates maximum tension with the wrist fully extended. Interestingly, the synergistic extensor carpi radialis longus (ECRL) also operates on its descending limb but over a much narrower sarcomere length range. This is due to the longer fibers and smaller wrist extension moment arm of the ECRL compared to the ECRB. Sarcomere lengths measured from wrist flexors are shorter compared to the extensors. Using a combination of intraoperative measurements on the flexor carpi ulnaris (FCU) and mechanical measurements of wrist muscles, joints and tendons, the general design of the prime wrist movers emerges: both muscle groups generate maximum force with the wrist fully extended. As the wrist flexes, force decreases due to extensor lengthening along the descending limb of their length–tension curve and flexor shortening along the ascending limb of their length–tension curve. The net result is a nearly constant ratio of flexor to extensor torque over the wrist range of motion and a wrist that is most stable in full extension. These experiments demonstrate the elegant match between muscle, tendon and joints acting at the wrist. Overall, the wrist torque motors appear to be designed for balance and control rather than maximum torque generating capacity.

Keywords: Sarcomere length; Wrist muscles; Musculoskeletal design

1. Introduction

Limb movement results from mechanical interaction between skeletal muscles, tendons and joints. The anatomy of these structures has been studied extensively at both the gross and microscopic levels [5,6,8,11,29]. Skeletal muscles are responsible for force generation during movement and have been shown to have a wide range of designs that appear to be matched to their functional tasks [3,15,27,32]. An added factor in understanding this system is that these muscles of varying design insert onto bones with a wide range of mechanical advantages yielding "torque motors" of designs that result from unique juxtaposition of muscle and joint properties.

Since relative muscle force is highly dependent on sarcomere length within the muscle, we have focused on sarcomere length measurements to provide insights into the design and function of the neuromuscular system. Prior studies of this sort in a variety of animal systems have yielded intriguing results. For example, it was demonstrated that fish fast and slow skeletal muscles operate near the peak of their power–velocity relationships at near optimal sarcomere length [24–26]. During locomotion in cats, medial gastrocnemius and soleus muscles are activated in such a manner as to exploit their metabolic and force generating properties [31,32]. Finally, frog skeletal muscles appear to be designed so as to maximize either power production during hopping [20] or moment transfer in the biarticular musculature [12,21].

* Corresponding author. Tel.: 001 619 552 8585, ext. 7016; fax: 001 619 552 4381; e-mail: rlieber@ucsd.edu

1050-6411/98/$19.00
PII: S1050-6411(97)00025-4

These studies suggest an impressive coordination among muscle, tendon and joint structural properties that are suited to the functional tasks. In some of these studies, understanding the design of the system was based on a description of the relationship between sarcomere length in a particular muscle and the joint on which it operates.

The studies reviewed here rely on intraoperative sarcomere length measurements in human upper extremity muscles combined with studies of cadaveric extremities to yield biomechanical models of human muscle function and to provide insights into the design and function of wrist muscles. We developed an intraoperative laser diffraction method to measure human muscle sarcomere length [7,16]. This method is noninjurious to the muscle and simply relies on the fact that laser light is diffracted by the striation pattern present in all skeletal muscles [17]. Since striation spacing is a direct manifestation of sarcomere length and sarcomere length is a good predictor of relative isometric muscle force, intraoperative sarcomere length measurements may provide insights into normal muscle and joint function.

2. Methods

2.1. Patient populations included

The subjects included in these studies were undergoing radial nerve release due to compression at the level of the supinator fascia (for combined extensor carpi radialis brevis [ECRB] and extensor carpi radialis longus [ECRL] measurements, $n = 7$) or surgical lengthening of the ECRB tendon for treatment of chronic lateral epicondylitis ("tennis elbow", $n = 5$). All patients received detailed instruction regarding experimental protocols. All procedures performed were approved by the Committee on the Use of Human Subjects at the University of Umeå and the University of California, San Diego.

2.2. Laser diffraction device

The device used was a 7 mW helium–neon laser (Melles-Griot, Model LHR-007, Irvine, CA, U.S.A.) onto which was mounted a custom component that permitted alignment between the laser beam and a small triangular prism (Melles-Griot Model PRA-001, Irvine, CA, U.S.A.). The laser beam was incident onto one of the short sides of the triangular prism, reflected off of the aluminum-coated surface of the other prism face, exiting 90° to the incident beam (Fig. 1). Thus the prism could be placed underneath a muscle bundle and transilluminated to produce a laser diffraction pattern[16].

The diffractometer was calibrated using diffraction gratings of 2.50 and 3.33 μm spacings placed directly upon the prism. Diffraction order spacings from the ± 2nd order were measured to the nearest 0.1 mm using dial calipers which corresponded to a sarcomere length resolution of about 0.05 μm. All sarcomere lengths were calculated using the + 2 to − 2 diffraction order spacing. Redundant measurements of + 1 to − 1 and + 3 to − 3 were also made to ensure calculation accuracy. Diffraction angle (θ) was calculated using the grating equation, $n\lambda = d \sin \theta$, where λ is the laser wavelength (0.632 μm), d is sarcomere length and n is diffraction order (second in all cases) and assuming that the zeroth order bisected the orders on either side.

2.3. Intraoperative protocols

2.3.1. ECRB and ECRL sarcomere length measurements

Immediately after administration of regional anesthesia, the distal ECRB and ECRL were exposed using a dorsoradial incision approximately 10 cm proximal to the radiocarpal joint. The overlying fascia was divided exposing the underlying muscle fibers. A small fiber bundle was isolated over a 1–2 cm region with the ends remaining intact. The region was chosen near the insertion site and the isolation occurred using delicate blunt dissection in a natural intramuscular fascial plane, with care not to overstretch muscle fibers. Since both muscles have characteristic appearance in this distal region, care was taken to isolate muscle fibers from the same region in all patients studied.

2.3.2. FCU sarcomere length measurements

After induction of general anesthesia, the muscle was exposed through a 3 cm longitudinal incision on the ulnar–palmar surface of the distal forearm. After exposure of the FCU by incision of the fascial sheath, a 5 mW He–Ne laser beam was directed into the distal portion of the FCU muscle fibers. With the elbow in 20° of flexion and the forearm supinated, FCU sarcomere length was measured with the wrist in full flexion, neutral, and full extension. Wrist joint angle was measured with a goniometer and was not identical in all subjects due to variations in anatomy and intraoperative positioning.

2.4. Biomechanical simulation

To predict the muscle force and wrist extension moment generated by the selected muscles the biomechanical model previously described [19] was implemented. This model was based on experimental measurement of prime wrist mover muscle architecture [14] and the mechanical properties of each wrist tendon [18]. Moment arms were then measured on cadaveric extremities [19]. Briefly, the forearm was mounted onto a mechanical jig and the distal humerus was secured by Steinman pins to vertical braces while an additional pin

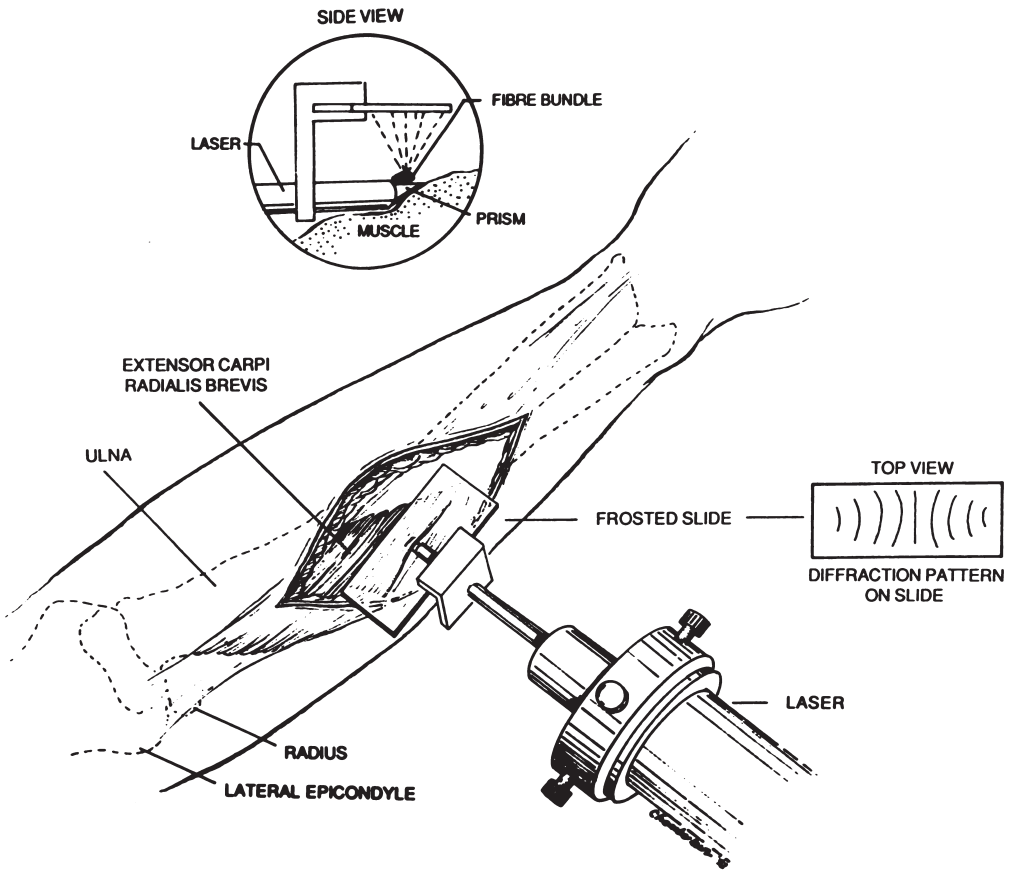

Fig. 1. Device used for intraoperative sarcomere length measurements. The He–Ne laser is aligned normal to the transmitting face of the prism for optimal transmission of laser power into the muscle. Second-order diffraction spacing was measured manually using calipers. Inset shows a transverse view of the illuminating prism placed beneath a muscle fibre bundle. Used with permission from [14].

engaged the middle third of the radius allowing forearm pronation and supination. Thirty-gauge stainless steel sutures were secured to the distal tendon stumps of each muscle (n = 25, five muscle-tendon units from five specimens) and routed subcutaneously over the muscle belly to the medial or lateral epicondyle recreating the line of force of each muscle. Steel sutures were then secured to toothed nylon cables and connected to non-backlash gears mounted to potentiometers as described by An et al. [1] and placed under 500 g tension. Tendon excursions were measured as the individual steel sutures rotated gears interfaced with potentiometers, providing voltage changes which corresponded linearly to suture and thus tendon excursion. A nonlinkage electrogoniometer (Penny and Giles, M series twin-axis goniometer) placed over the radiocarpal articulation measured joint angle in either the sagittal or coronal plane. Tendon excursion vs joint angle was measured and, using a specific stepwise regression procedure [4], data were fit and differentiated with respect to joint angle to yield moment arm equations.

Values obtained for flexion–extension moment arms of the prime wrist movers were:

$$r_{FCU}(\theta) = -14 + 0.028\theta$$

$$r_{ECU}(\theta) = 7.2 + 0.0022\theta^2 - 4.1 \times 10^{-9}\theta^5$$

$$r_{FCR}(\theta) = -15 + 0.082\theta$$

$$r_{ECRB}(\theta) = 16 + 0.16\theta + 0.00087\theta^2 - 0.000058\theta^3$$

$$r_{ECRL}(\theta) = 10 + 0.17\theta$$

where $r_i(\theta)$ moment arm is given in mm, wrist joint angle is in degrees, negative angles refer to wrist flexion and the subscript refers to the specific muscle. Using this procedure, each moment arm equation is permitted to include any polynomial terms and each muscle's equation is permitted to vary independent of other muscles.

Muscle properties were predicted based on architectural values obtained on cadaveric forearms [14] yielding muscle length–force curves scaled to fiber length and physiological cross-sectional area. The model predicts muscle moment as a function of joint angle using the known properties of the muscle and tendon and the appropriate moment arms. Sarcomere lengths predicted

by the model compare favorably to those obtained intraoperatively from the extensor carpi radialis brevis and FCU muscles [18].

3. Results

3.1. ECRB sarcomere lengths

The average flexed wrist joint angle was approximately − 50° while average extension angle was approximately + 50°. Therefore, sarcomere lengths were measured over a 100° range of wrist motion. With the wrist in full extension, sarcomere length was about 2.6 μm (Fig. 2) which was significantly shorter (and thus would develop about 50% of the tension) than the 3.4 μm sarcomere length measured in the flexed position. Sarcomere length with the joint in the neutral position was intermediate between these two values (3.0 μm) and significantly different than that observed in the flexed but not the extended position. In spite of the relatively large variations between individuals, sarcomere length–joint angle slopes remain remarkably constant. This may be due to the relatively poorly controlled elbow joint angle that may result in a sarcomere length offset.

Quantitative electron microscopy of human ECRB muscle tissue revealed actin filament lengths within half of the I-band (including half of the actin filament plus half of the Z-line) of 1.30 ± 0.027 μm while myosin filaments were 1.66 ± 0.027 μm long, yielding an optimal sarcomere length of 2.60–2.80 μm and a maximum sarcomere length for active force generation of 4.26 μm [16] compared to an optimal sarcomere length of 2.20 μm and a maximum sarcomere length for active force generation of 3.65 μm in frog and fish muscle [9,28].

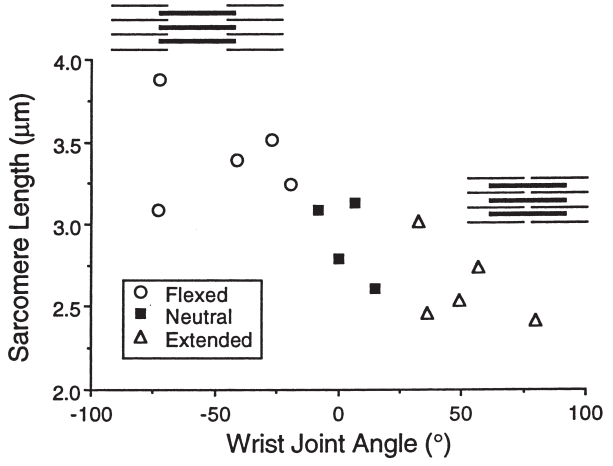

Fig. 2. Sarcomere length vs wrist joint angle relationship determined for the five experimental subjects. Negative angles represent wrist flexion relative to neutral while positive angles represent wrist extension. One-way ANOVA revealed a significant difference between wrist joint angles and sarcomere lengths in the three positions. (○) flexed angles, (■) neutral angles, (△) extended angles. Note that one point is missing from one subject at a neutral joint angle. Schematic sarcomeres placed upon data are based on quantitative measurement of filament lengths from human muscle biopsies. Used with permission from [14].

3.2. Average slope of ECRB and ECRL relationships

For all seven subjects studied the slope of the sarcomere length–joint angle curve (i.e. dSL/dϕ) was greater for the ECRB muscle compared to the ECRL. A relatively large degree of variability in dSL/dϕ was observed between subjects for both the ECRB and ECRL (Fig. 3). For example, ECRB dSL/dϕ ranged from − 5.4 to − 13.5 nm deg $^{-1}$ while those for the ECRL ranged from − 1.7 to − 11.2 nm deg $^{-1}$. Across all subjects, average dSL/dϕ for the ECRB was − 9.06 nm deg $^{-1}$ while that of the ECRL was about half of this value, or 4.69 nm deg^{-1}. We computed the ratio of dSL/dϕ between the ECRB and ECRL for each subject and averaged these values across subjects. This average dSL/dϕ ratio for the intraoperative sarcomere length data was 2.45.

4. Discussion

The main result of these studies is that sarcomere length operating range and moment arm are coordinated between muscles of the upper extremity in a way that suggests a balance between flexor and extensor moments.

4.1. Proposed design of the ECRB muscle

We collected the majority of our data on the ECRB muscle due to its accessibility and common involvement

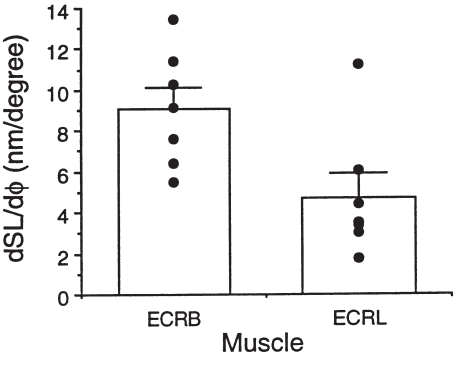

Fig. 3. Slope (dSL/dϕ) of the sarcomere length–joint angle relationship for the ECRB and ECRL muscles. Values are actually calculated as sarcomere length change per degree joint extension and are thus negative numbers since sarcomeres shorten with wrist extension. They are plotted as positive values for convenience. Used with permission from [15].

in surgical procedures. We found that human passive ECRB sarcomere lengths varied from 2.6 to 3.4 μm throughout the full range of wrist joint motion while active sarcomere lengths ranged from 2.44 to 3.33 μm. Active sarcomere lengths were calculated based on the measured compliance of the ECRB tendon [18] using an algorithm that permits physiological levels of sarcomere length change with muscle activation [13]. Given the measured actin filament length of about 1.3 μm and myosin filament length of 1.7 μm, these data suggest that the muscle operates primarily on the plateau and descending limb of its sarcomere length–tension curve (Fig. 4). Assuming that human muscles generate force as do frog skeletal muscles, optimal sarcomere length would occur between 2.60 and 2.80 μm which agrees well with the optimal sarcomere length of 2.64 to 2.81 μm predicted by Walker and Schrodt [30] based on filament length measurements. These data suggest that the ECRB muscle would develop near-maximal isometric force at full wrist extension, force would remain relatively constant as the sarcomeres lengthened "over" the plateau region, and then force would decrease to about 50% maximum at full wrist flexion. This result contrasts with the generally accepted notion that skeletal muscles generate maximum forces with the joint in a neutral position. We conclude, therefore, that muscle force change due to sarcomere length changes during joint rotation is "built-in" as part of the control in the musculoskeletal system and not simply a consequence of muscle microanatomy. Of course, the actual muscle force generated at a given angle depends not only on sarcomere length, but also on the number and firing frequency of motor units. Thus, the change in sarcomere length might be viewed as the "upper limit" for force production at a given joint angle.

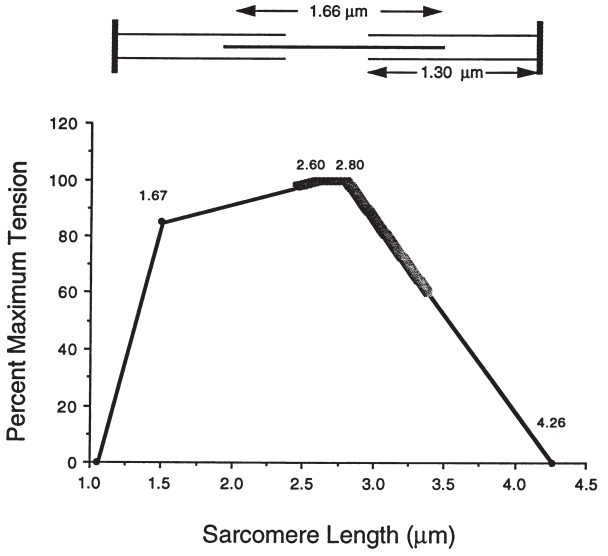

Fig. 4. Hypothetical length–tension curve obtained using measured filament lengths and assuming the sliding filament mechanism [10]. Shaded area represents sarcomere length change during wrist flexion (causing sarcomere length increase) and wrist extension (causing sarcomere length decrease). Top: schematic of filament lengths measured in the current study. Numbers over graph represent calculated inflection points based on filament lengths measured and a Z-disk width of 100 nm. Used with permission from [14].

4.2. Comparison between ECRB and ECRL muscles

Based on the measurement of sarcomere length changes of the ECRB and ECRL muscles with wrist joint rotation, we conclude that these muscles, while synergistic in terms of location and pattern of activation [2,22,23], have quite different anatomical designs that are predicted to produce different functional properties of the muscle–tendon–joint torque generating system.

To predict the expected ratio between $dSL/d\phi$ for the two muscles, muscle lengths and number of serial sar-

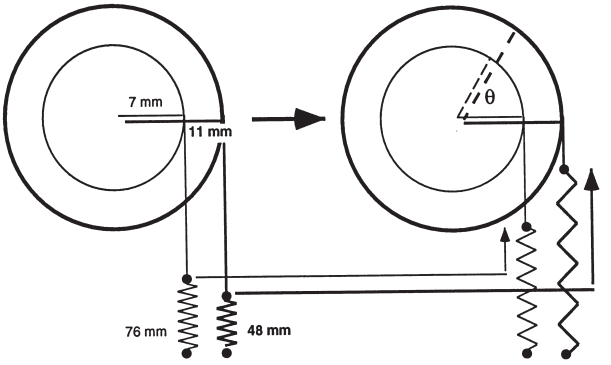

Fig. 5. Schematic diagram of the interrelationship between fiber length and moment arm for the ECRB and ECRL torque motors. The ECRB (bold print, thick lines) with its shorter fibers and longer moment arm changes sarcomere length about 2.5 times as much as the ECRL with its longer fibers and smaller moment arm. Used with permission from [15].

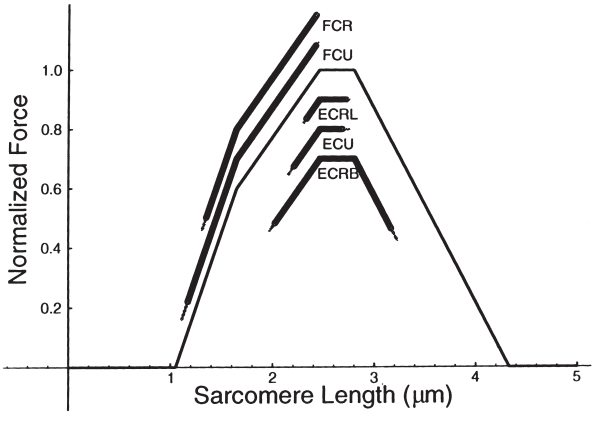

Fig. 6. Operating ranges of the wrist motors on the isometric sarcomere length–tension relation. Extensors operated primarily on the plateau region while the flexors operated predominantly along the ascending and steep ascending limbs. Mean sarcomere operating ranges were determined independently of the ensemble average muscle force– and torque–joint angle relations. Used with permission from [15].

comeres were obtained from upper extremity architecture data [14] while wrist extensor moment arms can be obtained from published kinematic data [19]. Sarcomere length change during wrist extension was thus modeled by integrating the moment arm equation over the range from about 40° of flexion to about 10° of extension (the average flexed and neutral positions respectively) for the ECRB. Given the relationship between muscle excursion (s), moment arm ($r(\phi)$) and angular rotation (ϕ) of $ds = r\,d\phi$, the ratio of sarcomere length changes with wrist extension for the two muscles is given by the expression:

$$\frac{dSL_B}{dSL_L} = \frac{r_B n_L}{r_L n_B}$$

where dSL is change of sarcomere length with joint rotation (i.e. $dSL/d\phi$), n is number of serial sarcomeres and B and L subscripts refer to values for the ECRB and ECRL respectively. The average moment arms for ECRB and ECRL across the same range measured experimentally were 11.37 and 6.94 respectively, while the serial sarcomere numbers were 27,143 and 17,143 respectively. Inserting these values into the above equation yields a sarcomere length change ratio of 2.57 which is close to the experimentally measured value of 2.45. This close agreement not only supports the modeling approach, it permits us to use this mechanical model to predict the joint moment of the wrist extensors reliably.

In the context of the current study, the major factor determining the properties of the torque motor is the ratio between the moment arm and the number of sarcomeres in series within the muscle. Using ordinary muscle architectural terminology, this would be

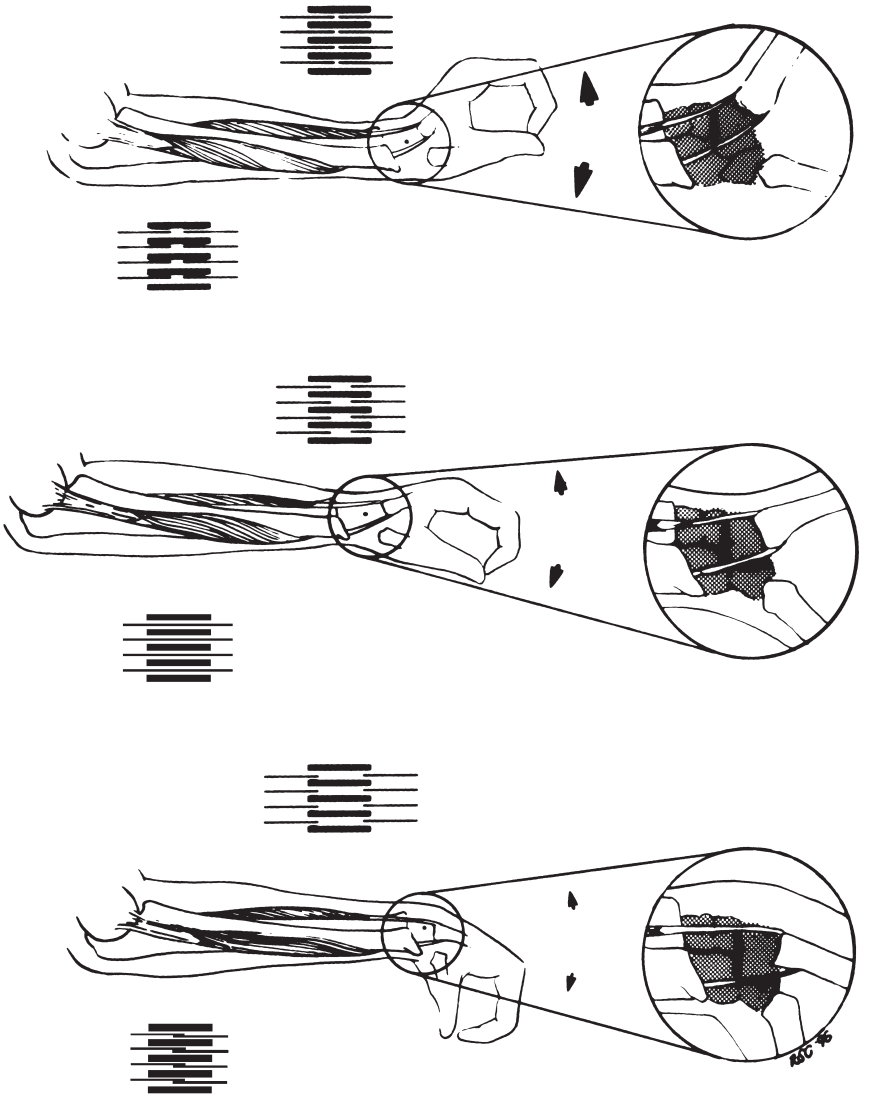

Fig. 7. Schematic depiction of sarcomere length, moment arm and moment in wrist flexors and extensors as the wrist moves throughout its range of motion.

expressed as the moment arm:fiber length ratio [33]. From a design point of view, high moment arm:fiber length ratio results in a torque motor where large fiber length changes produce large force changes during joint rotation and, thus, this motor would vary torque output greatly as the joint rotated. This is more or less the design of the ECRB torque motor for wrist extension motions, based on its relatively short fibers and large moment arm (Fig. 5). In contrast, the significantly longer fibers and smaller moment arm of the ECRL results in a torque motor with different functional properties. The ECRL-based motor retains a more constant torque output with joint rotation since, for a given amount of joint rotation, sarcomere length changes less (Fig. 3). In radial deviation, the situation is quite different. In this case, the increased ECRL radial deviation moment arm compared to the ECRB almost exactly matches their fiber length ratio [19]. Thus, for radial deviation movements, the sarcomere length change per radial deviation angle for both muscles is probably nearly equivalent. The fact that the ECRL has a substantial moment arm at the elbow while the ECRB has almost none does not seem to provide insight into its long-fibered design. The functional effect of such a design would be to maintain sarcomere length relatively constant in the ECRL with simultaneous wrist flexion and elbow extension while not affecting ECRB function.

4.3. Design of the wrist as a "torque motor"

Based on the relatively complete data set regarding wrist muscle and joint properties, a few general trends emerge. Wrist extensors are predicted to operate primarily on the plateau and descending limb of their sarcomere length–tension curve (Fig. 6) with all muscles generating maximal force in full extension. Only the ECRB was predicted to operate at sarcomere lengths corresponding to less than 80% P_o in the normal range of motion. Wrist flexors are predicted to operate predominantly on the shallow and steep ascending limbs of their length–tension curve with both flexors generating maximal force in full wrist extension (Fig. 6). Note that in full flexion, it is possible for wrist flexors to generate forces that are less than 50% P_o.

Such a design presents interesting implications for the design of the wrist as a torque motor. Both flexor and extensor muscle groups generate maximum force with the wrist fully extended. As the wrist extends, maximum isometric extensor force increases due to extensor *shortening* up the descending limb of the length–tension curve and maximum isometric flexor force increases due to flexor *lengthening* up the ascending limb of the length–tension curve. This effect is superimposed upon an increasing extensor moment arm as the extensor muscles elevate off of the wrist under the extensor retinaculum and a decreasing flexor moment arm as the flexors juxtapose the wrist from the flexor retinaculum. Combining the muscle and joint effects, extensor muscle force is amplified by an increasing extensor moment arm and flexor muscle force is attenuated by a decreasing flexor moment arm (Fig. 7). Interestingly, since the flexors as a group develop significantly greater force that the extensors (due to their larger physiological cross-sectional area), the net result is a nearly constant ratio of flexor to extensor torque over the wrist range of motion (Fig. 8). In fact, while at the muscle level, the flexors are considerably stronger than the extensors [3,14]; when including the wrist kinematics, extensor moment actually exceeds flexor moment. Additionally, wrist resistance to angular perturbation increases as the wrist is moved to full extension since both flexor and extensor moments increase in a similar fashion (Fig. 8). To summarize the results from these studies, coordination between muscle and joint properties results in a torque system that is balanced throughout the range of motion in spite of varying muscle force and joint moment arms. This balance is achieved at the expense of maximum moment generation at the wrist and, therefore, we conclude that this system is not simply designed to operate near maximum force as is often assumed in musculoskeletal models.

Acknowledgements

This work was supported by the Departments of Veteran Affairs, NIH Grant AR35192, the Swedish Medical Research Council (Project #11200) and the Medical Faculty at the Goteborg University. We are grateful to Drs Gordon Lutz and Reid Abrams for helpful discussions

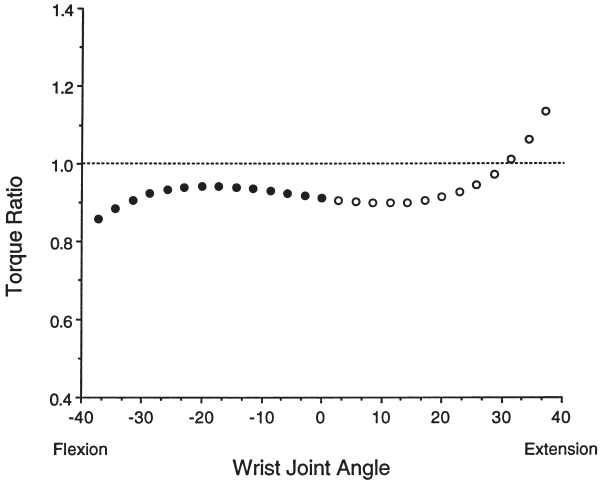

Fig. 8. Ratio between extension and flexion torque by the prime movers of the wrist calculated using the biomechanical model described. Note that, in spite of large differences in muscle forces, moment arms and sarcomere length operating ranges, the moments are nicely balanced throughout the range of motion. The wrist is in its most stable position in full extension where the moment produced by each muscle group is maximized.

and critical review of the manuscript. We also thank Thomas Burkholder for assistance in generating the biomechanical models. Finally, we thank Rebecca Chamberlain for skilful artistic rendering of Fig. 7.

References

[1] An KN, Ueba Y, Chao EY, Cooney WP, Linscheid RL. Tendon excursion and moment arm of index finger muscles. Journal of Biomechanics 1983;16–:419–25.
[2] Backdahl M, Carlsoo S. Distribution of activity in muscles acting on the wrist (an electromyographic study). Acta Morphologica Neerlando-Scandinavica 1961;4–:136–44.
[3] Brand PW, Beach RB, Thompson DE. Relative tension and potential excursion of muscles in the forearm and hand. Journal of Hand Surgery 1981;3–:209–19.
[4] Burkholder TJ, Lieber RL. Stepwise regression is an alternative to splines for analysing noisy data. Journal of Biomechanics 1996;29–:235–8.
[5] Butler, D. L., Grood, E. S., Noyes, F. R. and Zernicke, R. F., Biomechanics of ligaments and tendons. In *Exercise and Sport Sciences Reviews*. The Franklin Institute Press, Baltimore, MD, 1978, vol. 8, pp. 125–182.
[6] Ebashi, S., Maruyama, K. and Endo, M., *Muscle Contraction: its Regulatory Mechanisms*. Springer Verlag, New York, 1980.
[7] Friden J, Lieber RL. Physiological consequences of surgical lengthening of extensor carpi radialis brevis muscle–tendon junction for tennis elbow. Journal of Hand Surgery 1994;19A–:269–74.
[8] Gans, C., Fiber architecture and muscle function. In *Exercise and Sport Sciences Reviews*, Vol. 10. Franklin University Press, Lexington, MA, 1982, pp. 160–207.
[9] Gordon AM, Huxley AF, Julian FJ. Tension development in highly stretched vertebrate muscle fibres. Journal of Physiology (London) 1966;184–:143–69.
[10] Gordon AM, Huxley AF, Julian FJ. The variation in isometric tension with sarcomere length in vertebrate muscle fibres. Journal of Physiology (London) 1966;184–:170–92.
[11] Huxley AF. Muscular contraction. Journal of Physiology (London) 1974;243–:1–43.
[12] Lieber RL, Boakes JL. Sarcomere length and joint kinematics during torque production in the frog hindlimb. American Journal of Physiology 1988;254–:C759–68.
[13] Lieber RL, Brown CG, Trestik CL. Model of muscle–tendon interaction during frog semitendinosus fixed-end contractions. Journal of Biomechanics 1992;25–:421–8.
[14] Lieber RL, Fazeli BM, Botte MJ. Architecture of selected wrist flexor and extensor muscles. Journal of Hand Surgery 1990;15A–:244–50.
[15] Lieber RL, Jacobson MD, Fazeli BM, Abrams RA, Botte MJ. Architecture of selected muscles of the arm and forearm: anatomy and implications for tendon transfer. Journal of Hand Surgery 1992;17A–:787–98.
[16] Lieber RL, Loren GJ, Friden J. *In vivo* measurement of human wrist extensor muscle sarcomere length changes. Journal of Neurophysiology 1994;71–:874–81.
[17] Lieber RL, Yeh Y, Baskin RJ. Sarcomere length determination using laser diffraction. Effect of beam and fiber diameter. Biophysical Journal 1984;45–:1007–16.
[18] Loren GJ, Lieber RL. Tendon biomechanical properties enhance human wrist muscle specialization. Journal of Biomechanics 1995;28–:791–9.
[19] Loren GJ, Shoemaker SD, Burkholder TJ, Jacobson MD, Friden J, Lieber RL. Influences of human wrist motor design on joint torque. Journal of Biomechanics 1996;29–:331–42.
[20] Lutz GJ, Rome LC. Built for jumping: the design of the frog muscular system. Science 1994;263–:370–2.
[21] Mai MT, Lieber RL. A model of semitendinosus muscle sarcomere length, knee and hip joint interaction in the frog hindlimb. Journal of Biomechanics 1990;23–:271–9.
[22] McFarland GB, Krusen UL, Weathersby HT. Kinesiology of selected muscles acting on the wrist: electromyographic study. Archives of Physical Medicine and Rehabilitation 1962;43–:165–71.
[23] Riek S, Bawa P. Recruitment of motor units in human forearm extensors. Journal of Neurophysiology 1992;68–:100–8.
[24] Rome LC, Sosnicki AA. Myofilament overlap in swimming carp. II. Sarcomere length changes during swimming. American Journal of Physiology 1991;163–:281–95.
[25] Rome LC, Funke RP, Alexander RM, Lutz G, Aldridge H, Scott F, Freadman M. Why animals have different muscle fiber types. Nature 1988;335–:824–7.
[26] Rome LC, Swank D, Corda D. How fish power swimming. Science 1993;261–:340–3.
[27] Sacks RD, Roy RR. Architecture of the hindlimb muscles of cats: functional significance. Journal of Morphology 1982;173–:185–95.
[28] Sosnicki AA, Loesser KE, Rome LC. Myofilament overlap in swimming carp. I. Myofilament lengths of red and white muscle. American Journal of Physiology 1991;260–:C283–8.
[29] Squire, J., *The Structural Basis of Muscular Contraction*. Plenum Press, New York, 1981.
[30] Walker SM, Schrodt GR. I Segment lengths and thin filament periods in skeletal muscle fibers of the rhesus monkey and humans. Anatomical Record 1973;178–:63–82.
[31] Walmsley B, Proske U. Comparison of stiffness of soleus and medial gastrocnemius muscles in cats. Journal of Neurophysiology 1981;46–:250–9.
[32] Walmsley B, Hodgson JA, Burke RE. Forces produced by medial gastrocnemius and soleus muscles during locomotion in freely moving cats. Journal of Neurophysiology 1978;41–:1203–16.
[33] Zajac FE. How musculotendon architecture and joint geometry affect the capacity of muscle to move and exert force on objects: a review with application to arm and forearm tendon transfer design. Journal of Hand Surgery 1992;17A–:799–804.

Dr. Richard L. Lieber received a B.S. degree in animal physiology in 1978 and a Ph.D. (with honors) in 1982 in Biophysics from the University of California–Davis. He has been affiliated with the Veterans Affairs Hospital and the Department of Orthopedics and Rehabilitation in the University of California–San Diego since 1983. His research interest is in muscle physiology. He received the Talbot Award from the Biophysical Society in 1981, was Presidential Guest Speaker in the 1984 Academy of Cerebral Palsy and Developmental Disabilities, is a California Governor's Scholar since 1974 and is listed in the Harvard book. He is a member of the American College of Sports Medicine, the American Biophysical Society, American Physiological Society, IEEE, the Orthopedic Research Society, Society for Neuroscience, and RESNA.

Dr. Jan Friden is Professor of Hand Surgery at the Sahlgrenska University Hospital, Goteborg, Sweden. He received the M.D. 1978 and Ph.D. in Anatomy in 1983. His research interest is muscle physiology with special reference to muscle-tendon transfer in reconstructive hand surgery. He received the American Academy of Orthopaedic Surgeon's Kappa Delta Award in 1994. He currently serves as the Scientific Secretary of the Swedish Hand Society.